Carbohydrate Polymers 88 (2012) 713–718

Contents lists available at SciVerse ScienceDirect

Carbohydrate Polymers

journal homepage: www.elsevier.com/locate/carbpol

Preparation and characterization of thermal/pH-sensitive hydrogel from carboxylated nanocrystalline cellulose

Ruitao Cha [a,b,*], Zhibin He [b], Yonghao Ni [a,b]

[a] Tianjin Key Laboratory of Pulp and Paper, Tianjin University of Science and Technology, Tianjin 300457, China
[b] Limerick Pulp and Paper Centre, Department of Chemical Engineering, University of New Brunswick, Fredericton, New Brunswick, Canada E3B 5A3

ARTICLE INFO

Article history:
Received 13 November 2011
Received in revised form
20 December 2011
Accepted 7 January 2012
Available online 16 January 2012

Keywords:
Carboxylated nanocrystalline cellulose
N-Isopropyl acrylamide
Hydrogels
pH sensitive
Swelling behavior

ABSTRACT

Carboxylated nanocrystalline cellulose (CNCC) was used as a matrix material for the preparation of *N*-isopropyl acrylamide-based thermal/pH sensitive hydrogels. The resulting hydrogels' structure, morphology, thermal/pH-sensitive properties, swelling behavior and mechanical properties were investigated. The results indicated that the CNCC/PNIPAAm hydrogels exhibited the pH- and temperature-sensitivity. From its stress–strain curves, the hydrogels' stiffness increased obviously from the change of yield point when the amount of CNCC was increased. Scanning electron microscopy (SEM) supported the hypothesis that the added CNCC became an integral network of the hydrogels, which is responsible for the observed thermal/pH sensitivity and the improved strength.

1. Introduction

Hydrogels are crosslinked polymeric networks that have the ability to swell when suspended in water (Karlsson & Gatenholm, 1997). These absorbent polymers have a wide range of applications, such as sustained-release drug delivery systems, contact lenses, biosensors and much more (Meiring et al., 2004; Russell, Axel, Shields, & Pishko, 2001). In recent studies, the uses of natural polymers as a support matrix material have been investigated and showed favorable results (Van Vlierberghe, Dubruel, & Schacht, 2011).

Nano-crystalline cellulose (NCC) is the fundamental physical building block of wood cellulose and can be isolated from the crystalline regions of the fibre (Bai, Holbery, & Li, 2008; Jahan, Saeed, He, & Ni, 2011; Moon, Martini, Nairn, Simonsen, & Youngblood, 2011). These fibres have a number of appealing characteristics, such as optical, electrical and mechanical properties. When used in papermaking, NCC can alter the surface of paper leading to a change of the permeability, strength, flexibility and optical properties (Zoppe et al., 2010). NCC can also be used in other industrial applications, such as chemicals, cosmetics, pharmaceuticals and many more (Abitbol, Johnstone, Quinn, & Gray, 2011; Hasani, Cranston, Westman, & Gray, 2008; Simon, Kadiri, & Picard, 2008). Cellulose can be ideal support material for hydrogels because of its renewability, its good mechanical properties and its ability to be formed into many different structures (Rodriguez, Alvarez-Lorenzo, & Concheiro, 2003). It is an ideal carrier for many functional polymers, such as electro-conductive polymers (Ding, Qian, Shen, & An, 2010; Huang, Kang, & Ni, 2006), and functional chemicals for heavy metals such as Cr (VI) in water samples (Kong & Ni, 2009). In fact, the potential of making full use of lignocellulosic material, the so-called biorefinery strategy, has recently become the focus of many research activities (Shi, Fatehi, Xiao, & Ni, 2011; Van Heiningen, 2006; Zhu & Pan, 2010). Carboxylated nanocrystalline cellulose (CNCC) could be prepared from NCC (Follain, Marais, Montanari, & Vignon, 2010). Due to the large number of carboxylic acid groups found in CNCC, it is no surprise that it exhibits different characteristics at various pH levels.

Poly *N*-isopropylacrylamide is one of the most studied thermo-responsive polymers and has a lower critical solution temperature (LCST), ranging from 30 to 35 °C (Yoo, Sung, Lee, & Cho, 2000). The LCST is defined as the critical temperature at which a phase change is observed for the hydrogel, below the LCST, the components of a mixture are miscible. Due to the fact that the LCST is very close to the human physiological temperature of 37 °C, NIPAAm has been used in many studies involving controlled drug release (Ankareddi & Brazel, 2011; Geever & Higginbotham, 2011).

In this study, the incorporation of CNCC into NIPAAm-based hydrogels, and its effect on the resulting hydrogels, were investigated. The hypothesis is that the carboxylate groups of CNCC may

* Corresponding author at: Tianjin Key Laboratory of Pulp and Paper, Tianjin University of Science and Technology, Tianjin 300457, China. Tel.: +86 22 60601127; fax: +86 22 60602510.
E-mail address: ruitaocha@tust.edu.cn (R. Cha).

0144-8617/$ – see front matter © 2012 Elsevier Ltd. All rights reserved.
doi:10.1016/j.carbpol.2012.01.026

Table 1
Summary of the chemicals used for the preparation of the CNCC/PNIPAAm hydrogels.

	PNIPAAm ($GelCN_0$)	$GelCN_4$	$GelCN_7$	$GelCN_{10}$
CNCC (5 wt.%) (ml)	0	4	7	10
H_2O (ml)	25	21	18	15

impart to the hydrogel the desirable pH-responsive behavior, so that the advantageous characteristics of the carboxylate groups of the CNCC can be used to prepare a pH and thermal sensitive hydrogel. The addition of CNCC is also expected to improve the hydrogels' mechanical properties that are important for high water retaining capacity. The stimulus sensitive hydrogels exhibit a number of swelling properties in response to the environmental conditions. The chemical structure, morphology, swelling properties and compression strength of the gels were also studied systematically.

2. Experimental

2.1. Materials

CNCC was purchased from Biovision Technology Inc., and its carboxylate substitution degree at C6 was 0.1–0.2, as provided by the supplier. *N*-Isopropyl acrylamide (NIPAAm), *N*, *N*-methylenebisacrylamide (MBA), potassium persulfate (KPS), and 1, 2-di(dimethylamino)ethane (TMEDA) were purchased from Aldrich Chemical Co., Canada. Various pH buffer solutions were prepared using the combination of KH_2PO_4, K_2HPO_4, H_3PO_4, NaCl and NaOH solutions. Ionic strengths of the buffer solutions were adjusted to 0.1 M with NaCl solution. All other reagents were analytical grades and used without further purification.

2.2. Hydrogel preparation

A series of hydrogels were prepared with different mass ratios of CNCC to NIPAAm, following the method reported in the literature (Xu, Zhang, Cheng, Zhuo, & Kennedy, 2007). 1 g NIPAAm, 10 mg MBA (crosslinker), were dissolved in distilled water at room temperature, and then mixed with the specified amounts of the CNCC solution (the detailed conditions were given in Table 1). Then 0.020 ml KPS aqueous solution (16 mg/ml) was added as the initiator and 0.045 ml TEMED added as an accelerator to start the copolymerization, which was allowed to continue for 24 h at 15 °C. Thereafter, the hydrogel prepared was taken out and immersed in distilled water for 3 days at room temperature. During this period, the soaking water was replaced with fresh distilled water every several hours in order to wash away the residue. Here, the CNCC/PNIPAAm hydrogels thus obtained were labeled as GelCNx, where *x* represents the amount of CNCC; here the added CNCC becomes integral part of the hydrogel structure, and its uniform distribution is critical for the chemical/physical properties of the resulting hydrogel. The PNIPAAm hydrogel without CNCC was also prepared under the same procedures/conditions as those of the control, designated as PNIPAAm (or $GelCN_0$). The detailed chemicals compositions used are summarized in Table 1.

2.3. Characterizations

2.3.1. Fourier-transformed infrared spectroscopy (FT-IR)

FT-IR spectra were recorded using a S-100 FT-IR spectrometer (Perkin Elmer) and scanned from 4000 to 400 cm^{-1} in ATR mode and using KBr as supporting material; the samples were mixed with KBr powder at a weight ratio of 1:50. Thirty-two scans were taken for each sample with a resolution of 4 cm^{-1}.

2.3.2. Scanning electron microscopy (SEM)

The swollen hydrogel sample was first equilibrated in distilled water at room temperature, then quickly frozen in liquid nitrogen and freeze-dried in a Virtis Freeze Drier (Gardiner, NY) under vacuum at −45 °C for 3 days. After that, the freeze-dried hydrogel sample was fractured carefully in liquid nitrogen and then subjected to the SEM analysis using a scanning electron microscope (JSM-6400, JEOL, Japan). For the sample preparation, the hydrogel was gold-coated (Wang et al., 2008; Wang, Ni, Jahan, Liu, & Schafer, 2011).

2.3.3. Thermogravimetric analysis (TGA)

The thermal properties of hydrogel and CNCC were measured using thermogravimetric analysis (TGA). Decomposition profiles of TG were recorded at a heating rate of 10.0 °C/min between room temperature and 600.0 °C in nitrogen (its flow rate was 100 ml/min) (Wang et al., 2011; Zhang et al., 2009).

2.4. Temperature dependence of the equilibrium swelling ratio (ESR) of the hydrogels

The classical gravimetric method was used to measure the ESR of the hydrogels. For the temperature dependence of the ESR study, the hydrogel samples were equilibrated in water at a predetermined temperature ranging from 26 to 50 °C. The freeze-dried hydrogel sample (about 0.2 g) was soaked in an excessive amount of distilled water at each predetermined temperature for 7 h to reach the swelling equilibrium. The swollen hydrogels were filtered using a 100-mesh sieve and drained for 20 min to remove free water before weighing the mass of the swollen hydrogels (Zhang, Wu, Li, & Wang, 2005). The equilibrium water absorption can be calculated using Eq. (1):

$$\mathrm{ESR} = \frac{w_1 - w_0}{w_0} \quad (1)$$

In Eq. (1), ESR is the equilibrium water absorption, defined as grams of water per gram of sample; w_0 and w_1 are the weights of sample before and after swelling, respectively.

2.5. Evaluation of pH-sensitivity

The pH values were determined using a pH meter (OAKTON-300). The ESR result for each buffer solution at 26 °C was determined by following the same method as that in distilled water.

2.6. Swelling kinetics of the hydrogels

0.20 g of hydrogels was placed in 500 ml beaker and then 200 ml of aqueous solution was added. The swollen gel was filtered by a sieve after a pre-determined time interval and the water absorption at a given swelling time was determined from the mass changes before and after swelling. Three replicates were conducted and the averages were reported. The swelling ratio (SR) can be calculated using Eq. (2):

$$\mathrm{SR} = \frac{w_t - w_0}{w_0} \quad (2)$$

In Eq. (2), SR is the water absorption defined as grams of water per gram of sample; w_0 and w_t are the weights of sample before and after swelling for a specified time *t*, respectively.

2.7. Mechanical measurements

The mechanical property was measured using a Dynamic Mechanical Analyzer Q800 (TA Instruments). All mechanical measurements were conducted in a thermo-controlled container at

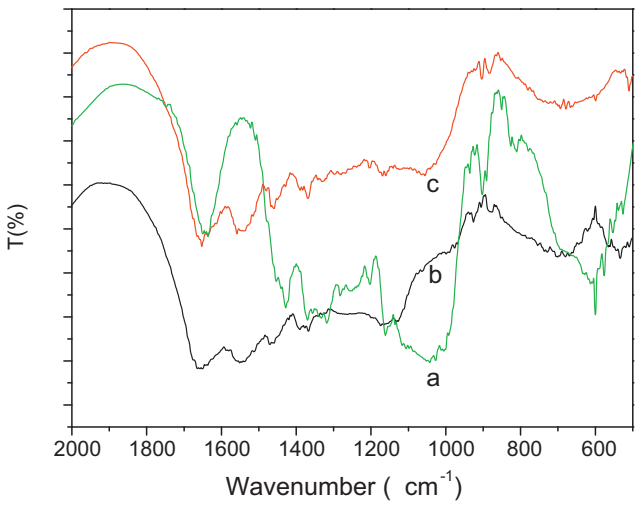

Fig. 1. FTIR Spectra of (a) CNCC, (b) PNIPAAm, and (c) $GelCN_{10}$ (CNCC/PNIPAAm).

24 °C. The compression test was measured using cylindrical swollen hydrogel specimens (13 by 6 mm). The compression rate was 0.5 N min^{-1} and the maximum force was 10 N (Yu et al., 2007).

3. Results and discussion

3.1. FTIR spectra

Shown in Fig. 1 are the FTIR spectra of CNCC, PNIPAAm and $GelCN_{10}$ (10% CNCC in PNIPAAm). For CNCC, the characteristic peaks are at 1061 cm^{-1}, 1410 and 1600 cm^{-1}, which are related to the stretching vibration of C—OH, symmetric stretching of —COO— groups and asymmetric stretching of —COO— groups, respectively. For PNIPAAm, the peaks at 1650 cm^{-1} and 1540 cm^{-1} can be attributed to N—C=O and N—H groups. In the FTIR spectrum of $GelCN_{10}$(CNCC/PNIPAAm), the peaks for C—OH at 1600 cm^{-1}, N—C=O at 1650 cm^{-1} and N—H at 1540 cm^{-1}, can all be identified. Therefore, it can be concluded that the CNCC/PNIPAAm hydrogel has the characteristic features of both CNCC and NIPAAm groups. In examining those of CNCC, PNIPAAM, and the CNCC/PNIPAAm hydrogel, one can note that the changes for C—OH, N—C=O and N—H were insignificant, indicating that there was no chemical reaction between CNCC and NIPAAM. As shown in the scheme of CNCC/PNIPAAm hydrogel preparation in Section 2.2, the CNCC was just physically dispersed in the hydrogel.

3.2. Morphology

The addition of CNCC to the CNCC/PNIPAAm hydrogel also changed its structure and morphology. Fig. 2 shows the SEM micrographs of CNCC, PNIPAAm hydrogel and CNCC/PNIPAAm hydrogel. It can be seen that CNCC contained aggregated fibrils of 100 nm in diameter and several hundreds of nanometers in length (Fig. 2a). The CNCC fibrils were also evident in the SEM of the CNCC/PNIPAAm hydrogel (Fig. 2c), which further supports the conclusion that the CNCC fibrils were uniformly dispersed in the hydrogel.

3.3. Thermal analysis

The thermal degradation behavior of the hydrogels was studied in the temperature range of 25–600 °C under a nitrogen atmosphere, and the results are presented in Fig. 3. The first phase of the weight loss (100–200 °C) is due to the evaporation of bound water, indicating that both hydrogels were hygroscopic. This is consistent with previous results reported in the literature (Schild, 1996). For the PNIPAAm hydrogel, the vast majority of the weight loss occurred at higher than 250 °C, with the maximum decomposition rate at 386 °C. Beyond 315 °C, the backbone of the PNIPAAm started to degrade corresponding to a weight loss of 81%. For CNCC, the majority of the weight loss occurred in the range of 268–362 °C, and two maximum decomposition temperatures were observed in the DTG curves: one at around 242 °C and the other at about 317 °C. This thermal characteristic was similar to those for the acid treated NCC samples (Wang, Ding, & Cheng, 2007). And for the CNCC/PNIPAAm hydrogel, its maximum decomposition rate was at 397 °C. The last degradation temperature of the hydrogels was due to random chain scission of PNIPAAm. The CNCC/PNIPAAm hydrogel was thermally more stable than the PNIPAAm crosslinked gel, most likely due to the presence of CNCC, which resulted in more ordered structure of the CNCC/PNIPAAm hydrogel as indicated from the SEM images (Fig. 2(c)).

3.4. Thermal sensitivity

Similar to the PNIPAAm hydrogel, the CNCC/PNIPAAm hydrogel exhibited a typical volume phase transition (VPT) behavior responsive to a temperature change, due to the presence of the NIPAAm polymer chains. The VPT behavior stemmed from the LCST characteristic of hydrogels. The LCST of hydrogel is the lower critical temperature at which phase change is observed for the hydrogel. Below the LCST, the NIPAAm polymer chains tend to form a random coil conformation, causing the hydrogel to swell. When

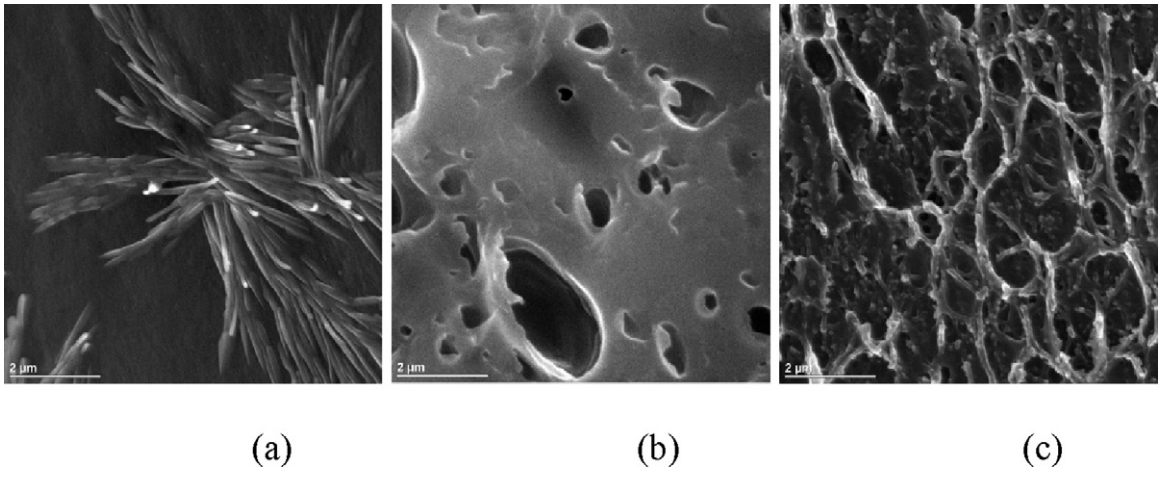

Fig. 2. SEM images of freeze-dried (a) CNCC, (b) PNIPAAm hydrogel, and (c) CNCC/PNIPAAm hydrogel.

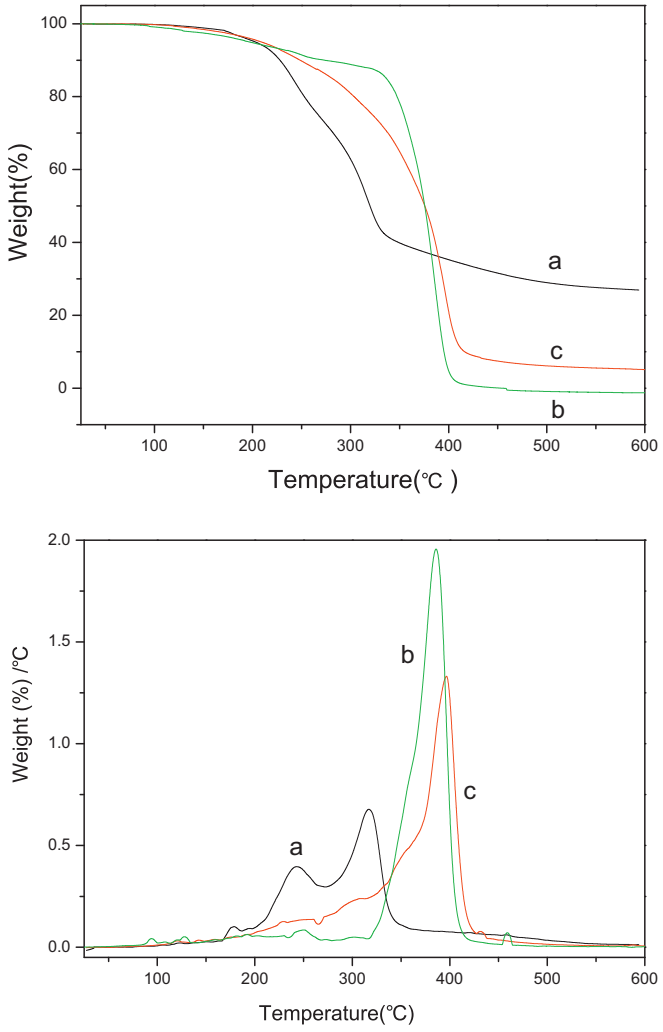

Fig. 3. TG (top) and DTG (bottom) curves of (a) CNCC, (b) PNIPAAm and (c) CNCC/PNIPAAm hydrogels.

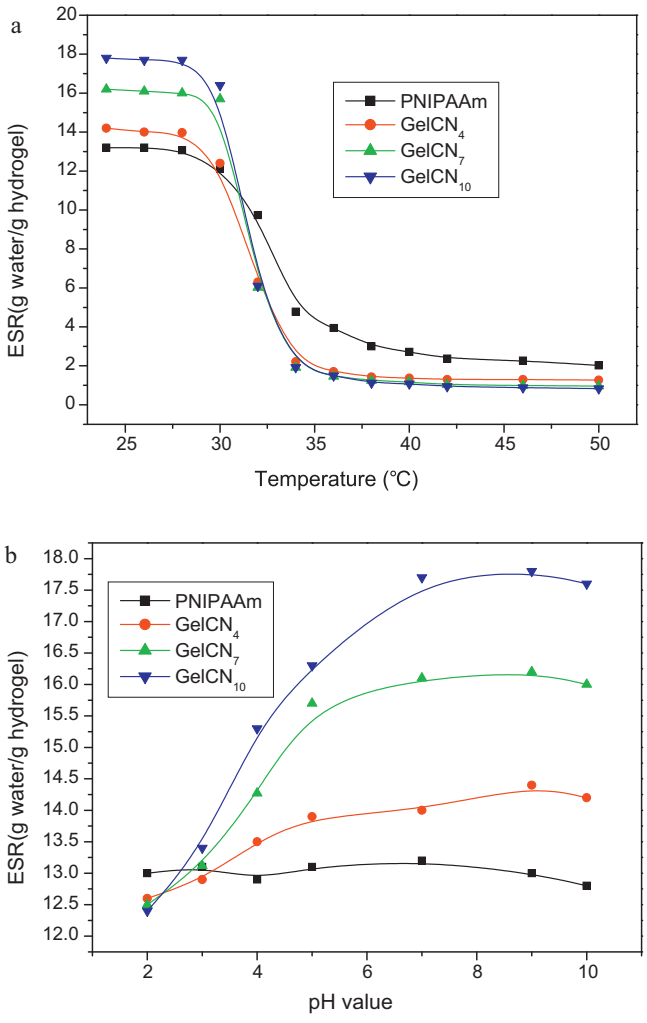

Fig. 4. ESR of hydrogels as functions of (a) temperature or (b) pH at 26 °C.

the temperature is increased above the LCST, the random NIPAAm polymer coils collapse, causing the hydrogel to shrink. At a low temperature (<28 °C) the swollen hydrogels were homogeneous and transparent. At a high temperature (>40 °C), the hydrogels shrank and became cloudy, indicating the occurrence of the volume phase transition. The shrunk hydrogels can be re-swollen in water and became transparent again when they were below the LCST. The equilibrium swelling ratio (ESR) is one of the most important parameters for evaluating hydrogels because it can illustrate the temperature-sensitive properties of hydrogels.

The swelling behavior of the prepared hydrogels in distilled water at different temperatures was determined and the results are shown in Fig. 4(a). All of the CNCC/PNIPAAm hydrogels demonstrated similar thermo-responsive profiles. Below the LCST, the hydrogels exhibited swollen states with high swelling ratios. As the external temperature increased, the swelling ratios of the hydrogels decreased, due to the shrinking of hydrogel, resulting from the collapse of the NIPAAm polymer coils.

Moreover, at the same temperature (below the LCST), the ESR increases with the increase of the CNCC content in the hydrogel. For example, $GelCN_{10}$ had the highest ESR (17.8 g/g) at 24 °C, while the ESR for $GelCN_7$, $GelCN_4$ and $GelCN_0$ (PNIPAAm hydrogel) was 16.2, 14.2, and 13.2 g/g, respectively. These results indicate that the water holding capacities of the hydrogels increased significantly with the addition of CNCC. It is easier for CNCC to form hydrogen bonds with water molecules using the carboxyl groups (Dumitriu, Mitchell, & Vasile, 2011); this can be explained by the improved hydrogel network during the polymerization process and the increase of the specific surface area, as evidenced from the SEM results in Fig. 2.

3.5. *pH sensitivity*

The carboxylic groups on the surface of CNCC can render the CNCC/PNIPAAm hydrogels pH-sensitive properties. As shown in Fig. 4(b), the ESR of the CNCC/PNIPAAm hydrogels increased markedly with the increase of pH. In contrast, the ESR for the PNIPAAm hydrogel was essentially pH independent. The pH sensitivity of the CNCC/PNIPAAm hydrogels also increased significantly with the increase of the CNCC content added in the polymerization process, as shown in Fig. 4(b). This is particularly true in the pH range of 3.0–7.0.

The —COO^- and —COOH functional groups on the CNCC nano fibres can be interchanged, depending on the pH of the medium. The carboxylic functional groups of the CNCC had a pK_a of about 3.2. When the system pH was lower than the pK_a, most of the carboxylic groups were in their —COOH form. Strong hydrogen-bonding was formed between the —OH and —COOH groups, which impairs the diffusion of water into its structure (Wang & Wang, 2010). As a result, the ESR was reduced. When the pH was higher than the pK_a, most of the —COOH groups are dissociated, and in

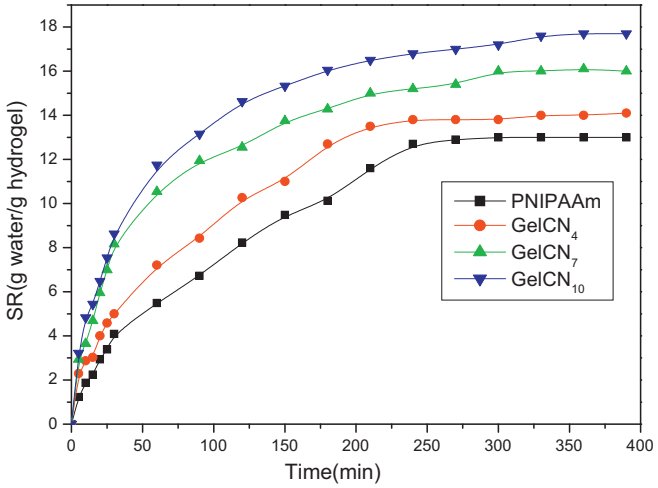

Fig. 5. Swelling kinetics of the hydrogels in distilled water at 26 °C.

the —COO^- form, leading to the significant decrease in the hydrogen bonds (Hoogendam et al., 1998; Lu, Liu, Ni, & Gao, 2010; Zhao et al., 2009). Due to the increase in the number of negatively charged —COO^- groups, the electrostatic repulsion became dominant, which facilitated the diffusion of water molecules into the network to swells the hydrogel. These results are in good agreement with a previous study (Shi, Zhang, Ma, & Yi, 2007), in which the graft copolymer of *N*-isopropylacrylamide (NIPAAm) on carboxymethylcellulose (CMC) was investigated with respect to their pH behavior in aqueous solution. The significant change of the ESR in response to the pH change of the external buffer solution demonstrated the pH-sensitive characteristic of the CNCC/PNIPAAm hydrogels.

3.6. Swelling kinetics

Fig. 5 shows the swelling ratio (SR) as a function of time for the PNIPAAm and CNCC/PNIPAAm hydrogels in distilled water at 26 °C. Initially the rates of swelling increased rapidly. The increase slowed down at 25 min, and started to level off at about 200 min. The equilibrium swelling was achieved at about 7 h. It can be seen that the SR values of the CNCC/PNIPAAm hydrogels was significantly higher than that for the control PNIPAAm hydrogel, and it increased with increasing the CNCC content in the hydrogels. The swelling of the $GelCN_{10}$ is faster than that of the other three gels; this is due to the hydrophilic nature of the carboxyl groups in CNCC. The increasing hydrogen bonds among water molecules and CNCC resulted in a faster swelling of the $GelCN_{10}$ hydrogels (Zhang, Zhong, Zhang, Chen, & Zhao, 2010). Again, these results support the conclusion that the addition of CNCC enhanced the swelling behavior of the hydrogels.

3.7. Strength property

Fig. 6 shows the results of mechanical strength analysis of the CNCC/PNIPAAm hydrogels. It can be seen from the strain/stress curve that the yield point of the hydrogel was 0.8 (PNIPAAm), 2.6 ($GelCN_4$), 3.5 ($GelCN_7$) and 4.7 ($GelCN_{10}$), respectively. The strain/stress curve of PNIPAAm hydrogel (a) was linear after the static force reached 0.4 N, which is in agreement with Hook's law, indicating that the compression is an elastic deformation process. The PNIPAAm hydrogel fractured when the static compressing force was 0.8 N and the strain was −22%. Then the PNIPAAm hydrogel compressed at a slower speed; it collapsed at the strain of −36%.

With the addition of CNCC, it can also be seen that the strain of the hydrogels increased from 22% to 42%(b), 46%(c) and 50%(d)

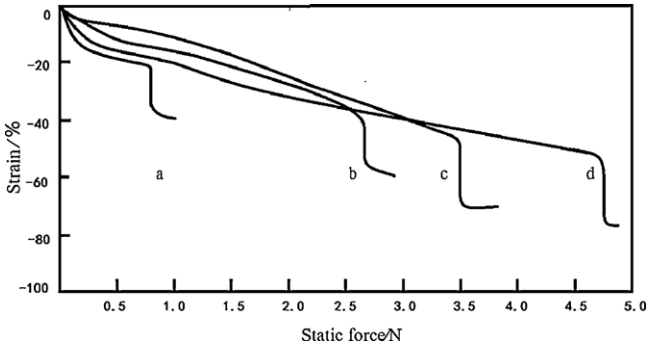

Fig. 6. Mechanical properties of hydrogels: (a) PNIPAAm; (b) $GelCN_4$; (c) $GelCN_7$; and (d) $GelCN_{10}$.

at the yield point; and increased from 36% to 58%(b), 68%(c) and 77%(d) when the hydrogels were compressed to collapse. These results reveal that the hydrogels' mechanical strength was significantly improved with the addition of CNCC, the higher the CNCC content, the higher the strength property. It is evident that the CNCC increased the stiffness and toughness of the hydrogels by forming network structure in the hydrogels, as supported from the SEM results (Fig. 2). CNCC was the backbone of the hydrogel matrix, which facilitates water holding capacity of the resultant hydrogel (Chang, Duan, & Zhang, 2009; Chang, Han, & Zhang, 2011). Also, the mechanical properties of CNCC/PNIPAAm hydrogels may be controlled by adjusting the content of CNCC to be consistent with their application.

4. Conclusions

The pH/thermal sensitive hydrogels were successfully synthesized using NIPAAm monomer and carboxylated nanocrystalline cellulose (CNCC). The CNCC/PNIPAAm hydrogels' structure, morphology, thermal/pH-sensitive property, swelling property and mechanical strength were investigated. Results showed that the resultant hydrogels exhibited both pH-sensitive and thermal-sensitive properties. Swelling ratios of the hydrogels increased with the increase of CNCC at the same temperature. SEM images supported the conclusion that the CNCC nano-fibrils were uniformly dispersed in the hydrogel without agglomeration. The introduction of the CNCC to the hydrogel structure also significantly improved its mechanical properties.

References

Abitbol, T., Johnstone, T., Quinn, T. M., & Gray, D. G. (2011). Reinforcement with cellulose nanocrystals of poly(vinyl alcohol) hydrogels prepared by cyclic freezing and thawing. *Soft Matter*, *7*, 2373–2379.

Ankareddi, I., & Brazel, C. S. (2011). Development of a thermosensitive grafted drug delivery system-synthesis and characterization of NIPAAm-based grafts and hydrogel structure. *Journal of Applied Polymer Science*, *120*, 1597–1606.

Bai, W., Holbery, J., & Li, K. C. (2008). A technique for production of nanocrystalline cellulose with a narrow size distribution. *Cellulose*, *16*, 455–465.

Chang, C. Y., Duan, B., & Zhang, L. N. (2009). Fabrication and characterization of novel macroporous cellulose-alginate hydrogels. *Polymer*, *50*, 5467–5473.

Chang, C. Y., Han, K., & Zhang, L. N. (2011). Structure and properties of cellulose/poly(*N*-isopropylacrylamide) hydrogels prepared by IPN strategy. *Polymer for Advanced Technology*, *22*, 1329–1334.

Ding, C., Qian, X., Shen, J., & An, X. (2010). Preparation and characterization of conductive paper via in situ polymerization of pyrrole. *Bioresearch*, *5*(1), 303–315.

Dumitriu, R. P., Mitchell, G. R., & Vasile, C. (2011). Multi-responsive hydrogels based on N-isopropylacrylamide and sodium alginate. *Polymer International*, *60*, 222–233.

Follain, N., Marais, M. F., Montanari, S., & Vignon, M. R. (2010). Coupling onto surface carboxylated cellulose nanocrystals. *Polymer*, *51*, 5332–5344.

Geever, L. M., & Higginbotham, C. L. (2011). Temperature-triggered gelation and controlled drug release via NIPAAm/NVP-based hydrogels. *Journal of Materials Science*, 3233–3240.

Hasani, M., Cranston, E. D., Westman, G., & Gray, D. G. (2008). Cationic surface functionalization of cellulose nanocrystals. *Soft Matter*, *4*, 2238–2244.

Hoogendam, C. W., de Keizer, A., Stuart, M. A. C., Bijsterbosch, B. H., Smit, J. A. M., van Dijk, J. A. P. P., et al. (1998). Persistence length of carboxymethyl cellulose as evaluated from size exclusion chromatography and potentiometric titrations. *Macromolecules*, *31*, 6297–6309.

Huang, B., Kang, G. J., & Ni, Y. (2006). Preparation of conductive paper by in situ polymerization of pyrrole in a pulp fibre system. *Pulp & Paper – Canada*, *107*(2), 38–42.

Jahan, M. S., Saeed, A., He, Z., & Ni, Y. H. (2011). Jute as raw material for the preparation of microcrystalline cellulose. *Cellulose*, *18*(2), 451–459.

Karlsson, J. O., & Gatenholm, P. (1997). Preparation and characterization of cellulose-supported HEMA hydrogels. *Polymer*, *38*, 4727–4731.

Kong, F., & Ni, Y. (2009). Determination of Cr(VI) concentration in diluted samples based on the paper test strip method. *Water Science and Technology*, *60*(12), 3083–3089.

Lu, S. Y., Liu, M. Z., Ni, B. L., & Gao, C. M. (2010). A novel pH- and thermo-sensitive PVP/CMC semi-IPN hydrogel: Swelling, phase behavior, and drug release study. *Journal of Polymer Science Part B – Polymer Physics*, *48*, 1749–1756.

Meiring, J. E., Schmid, M. J., Grayson, S. M., Rathsack, B. M., Johnson, D. M., Kirby, R., et al. (2004). Hydrogel biosensor array platform. *Chemistry of Materials*, *16*, 5574–5580.

Moon, R. J., Martini, A., Nairn, J., Simonsen, J., & Youngblood, J. (2011). Cellulose nanomaterials review: Structure, properties and nanocomposites. *Chemical Society Reviews*, *40*, 3941–3994.

Rodriguez, R., Alvarez-Lorenzo, C., & Concheiro, A. (2003). Cationic cellulose hydrogels: Kinetics of the cross-linking process and characterization as pH-/ion-sensitive drug delivery systems. *Journal of Controlled Release*, *86*, 253–265.

Russell, R. J., Axel, A. C., Shields, K. L., & Pishko, M. V. (2001). Mass transfer in rapidly photopolymerized poly(ethylene glycol) hydrogels used for chemical sensing. *Polymer*, *42*, 4893–4901.

Schild, H. G. (1996). Thermal decomposition of PNIPAAM: TGA-FTIR analysis. *Journal of Polymer Science Part A – Polymer Chemistry*, *34*(11), 2259–2262.

Shi, H. Y., Zhang, L. M., Ma, Y. Q., & Yi, J. Z. (2007). Synthesis and characterization of water-soluble cellulose derivatives with thermo- and pH-sensitive functional groups. *Journal of Macromolecular Science Part A – Pure and Applied Chemistry*, *44*, 1109–1113.

Shi, H., Fatehi, P., Xiao, H., & Ni, Y. (2011). A combined acidification/PEO flocculation process to improve the lignin removal from the pre-hydrolysis liquor of kraft-based dissolving pulp production process. *Bioresource Technology*, *102*(8), 5177–5182.

Simon, D., Kadiri, Y., & Picard, G. (2008). Nano cellulose crystallites: Optical, photonic and electro-magnetic properties. In *NSTI NANOTECH 2008, technical proceedings (Vol. 1)* (pp. 840–843).

Van Heiningen, A. (2006). Converting a kraft pulp mill into an integrated forest biorefinery. *Pulp & Paper – Canada*, *107*(6), 38–43.

Van Vlierberghe, S., Dubruel, P., & Schacht, E. (2011). Biopolymer-based hydrogels as scaffolds for tissue engineering applications: A review. *Biocromolecules*, *12*, 1387–1408.

Wang, W. D., & Wang, A. Q. (2010). Nanocomposite of carboxymethyl cellulose and attapulgite as a novel pH-sensitive superabsorbent: Synthesis, characterization and properties. *Carbohydrate Polymers*, *82*, 83–91.

Wang, N., Ding, E. Y., & Cheng, R. S. (2007). Thermal degradation behaviors of spherical cellulose nanocrystals with sulfate groups. *Polymer*, *48*(12), 3486–3493.

Wang, B., Xu, X. D., Wang, Z. C., Cheng, S. X., Zhang, X. Z., & Zhu, R. X. (2008). Synthesis and properties of pH and temperature sensitive P(NIPAAm-co-DMAEMA) hydrogels. *Colloid and Surfaces B – Biointerfaces*, *64*, 34–41.

Wang, H., Ni, Y., Jahan, M. S., Liu, Ze., & Schafer, T. (2011). Stability of cross-linked acetic acid lignin-containing polyurethane. *Journal of Thermal Analysis and Calorimetry*, *103*(1), 293–302.

Xu, X. D., Zhang, X. Z., Cheng, S. X., Zhuo, R. X., & Kennedy, J. F. (2007). A strategy to introduce the pH sensitivity to temperature sensitive PNIPAAm hydrogels without weakening the thermosensitivity. *Carbohydrate Polymers*, *68*, 416–423.

Yoo, M. K., Sung, Y. K., Lee, Y. M., & Cho, C. S. (2000). Effect of polyelectrolyte on the lower critical solution temperature of poly(*N*-isopropyl acrylamide) in the poly(NIPAAm-co-acrylic acid) hydrogel. *Polymer*, *41*, 5713–5719.

Yu, J., Liu, S. X., Fang, Y., Wang, Y. J., Chen, F. Q., & Zhang, Z. Y. (2007). Synthesis and characterization of nano-TiO_2/poly(*N*-isopropylacrylamide) composite hydrogel. *Acta Chimica Sinica*, *65*, 2437–2442.

Zhang, Y. X., Wu, F. P., Li, M. Z., & Wang, E. J. (2005). pH switching on-off semi-IPN hydrogel based on cross-linked poly(acrylamide-co-acrylic acid) and linear polyallyamine. *Polymer*, *46*, 7695–7700.

Zhang, H. F., Zhong, H., Zhang, L. L., Chen, S. B., Zhao, Y. J., & Zhu, Y. L. (2009). Synthesis and characterization of thermosensitive graft copolymer of *N*-isopropylacrylamide with biodegradable carboxymethylchitosan. *Carbohydrate Polymers*, *77*, 785–790.

Zhang, H. F., Zhong, H., Zhang, L. L., Chen, S. B., & Zhao, Y. J. (2010). Modulate the phase transition temperature of hydrogels with both thermosensitivity and biodegradability. *Carbohydrate Polymers*, *79*, 131–136.

Zhao, C., Zhuang, X., He, P., Xiao, C., He, C., Sun, J., et al. (2009). Synthesis of biodegradable thermo- and pH-responsive hydrogels for controlled drug release. *Polymer*, *50*, 4308–4316.

Zhu, J. Y., & Pan, X. J. (2010). Woody biomass pretreatment for cellulosic ethanol production: Technology and energy consumption evaluation. *Bioresource Technology*, *101*(13), 4992–5002.

Zoppe, J. O., Habibi, Y., Rojas, O. J., Venditti, R. A., Johansson, L. S., Efimenko, K., et al. (2010). Poly(*N*-isopropylacrylamide) brushes grafted from cellulose nanocrystals via surface-initiated single-electron transfer living radical polymerization. *Biomacromolecules*, *11*, 2683–2691.